NASA/TM—2013-216581

Structural Benchmark Creep Testing for Microcast MarM-247 Advanced Stirling Convertor E2 Heater Head Test Article SN18

David L. Krause
Glenn Research Center, Cleveland, Ohio

Ethan J. Brewer
The Ohio State University, Columbus, Ohio

Ralph J. Pawlik
University of Toledo, Toledo, Ohio

September 2013

NASA STI Program . . . in Profile

Since its founding, NASA has been dedicated to the advancement of aeronautics and space science. The NASA Scientific and Technical Information (STI) program plays a key part in helping NASA maintain this important role.

The NASA STI Program operates under the auspices of the Agency Chief Information Officer. It collects, organizes, provides for archiving, and disseminates NASA's STI. The NASA STI program provides access to the NASA Aeronautics and Space Database and its public interface, the NASA Technical Reports Server, thus providing one of the largest collections of aeronautical and space science STI in the world. Results are published in both non-NASA channels and by NASA in the NASA STI Report Series, which includes the following report types:

- TECHNICAL PUBLICATION. Reports of completed research or a major significant phase of research that present the results of NASA programs and include extensive data or theoretical analysis. Includes compilations of significant scientific and technical data and information deemed to be of continuing reference value. NASA counterpart of peer-reviewed formal professional papers but has less stringent limitations on manuscript length and extent of graphic presentations.

- TECHNICAL MEMORANDUM. Scientific and technical findings that are preliminary or of specialized interest, e.g., quick release reports, working papers, and bibliographies that contain minimal annotation. Does not contain extensive analysis.

- CONTRACTOR REPORT. Scientific and technical findings by NASA-sponsored contractors and grantees.

- CONFERENCE PUBLICATION. Collected papers from scientific and technical conferences, symposia, seminars, or other meetings sponsored or cosponsored by NASA.

- SPECIAL PUBLICATION. Scientific, technical, or historical information from NASA programs, projects, and missions, often concerned with subjects having substantial public interest.

- TECHNICAL TRANSLATION. English-language translations of foreign scientific and technical material pertinent to NASA's mission.

Specialized services also include creating custom thesauri, building customized databases, organizing and publishing research results.

For more information about the NASA STI program, see the following:

- Access the NASA STI program home page at *http://www.sti.nasa.gov*

- E-mail your question to *help@sti.nasa.gov*

- Fax your question to the NASA STI Information Desk at 443–757–5803

- Phone the NASA STI Information Desk at 443–757–5802

- Write to:
  STI Information Desk
  NASA Center for AeroSpace Information
  7115 Standard Drive
  Hanover, MD 21076–1320

NASA/TM—2013-216581

Structural Benchmark Creep Testing for Microcast MarM-247 Advanced Stirling Convertor E2 Heater Head Test Article SN18

David L. Krause
Glenn Research Center, Cleveland, Ohio

Ethan J. Brewer
The Ohio State University, Columbus, Ohio

Ralph J. Pawlik
University of Toledo, Toledo, Ohio

National Aeronautics and
Space Administration

Glenn Research Center
Cleveland, Ohio 44135

September 2013

Acknowledgments

The authors appreciate the inspiring leadership and management at GRC provided by Scott Benson, Dick Shaltens, Lee Mason, Wayne Wong, Jeff Schreiber, Scott Wilson, and Lanny Thieme, as well as the full support and technical management of Drs. Ajay Misra, Steven Arnold, and Michael Nathal. The authors also thank Dr. Sreeramesh Kalluri for his expert experimental advice, development of analytical methods, and steadfast reporting of technical progress; Dr. Randy Bowman for his continued metallurgical help and expertise; Ashwin Shah and Igor Korovaichuk, Sest, Inc. for their tireless efforts in modeling, analysis, and development of reliability and life assessment methodologies; and Frank Bremenour for his technical collaboration and able laboratory support for heater head benchmark testing. The Science Mission Directorate at NASA Headquarters provided funding to complete the work described herein, and the authors truly are grateful for that enduring commitment.

Level of Review: This material has been technically reviewed by technical management.

Available from

NASA Center for Aerospace Information
7115 Standard Drive
Hanover, MD 21076–1320

National Technical Information Service
5301 Shawnee Road
Alexandria, VA 22312

Available electronically at http://www.sti.nasa.gov

Structural Benchmark Creep Testing for Microcast MarM-247 Advanced Stirling Convertor E2 Heater Head Test Article SN18

David L. Krause
National Aeronautics and Space Administration
Glenn Research Center
Cleveland, Ohio 44135

Ethan J. Brewer
The Ohio State University
Columbus, Ohio 43210

Ralph J. Pawlik
University of Toledo
Toledo, Ohio 43606

Abstract

This report provides test methodology details and qualitative results for the first structural benchmark creep test of an Advanced Stirling Convertor (ASC) heater head of ASC-E2 design heritage. The test article was recovered from a flight-like Microcast MarM-247 heater head specimen previously used in helium permeability testing. The test article was utilized for benchmark creep test rig preparation, wall thickness and diametral laser scan hardware metrological developments, and induction heater custom coil experiments. In addition, a benchmark creep test was performed, terminated after one week when through-thickness cracks propagated at thermocouple weld locations. Following this, it was used to develop a unique temperature measurement methodology using contact thermocouples, thereby enabling future benchmark testing to be performed without the use of conventional welded thermocouples, proven problematic for the alloy. This report includes an overview of heater head structural benchmark creep testing, the origin of this particular test article, test configuration developments accomplished using the test article, creep predictions for its benchmark creep test, qualitative structural benchmark creep test results, and a short summary.

1.0 Introduction

The NASA Glenn Research Center (GRC) has provided life and reliability verification and advanced development for several technologies used in the Advanced Stirling Radioisotope Generator (ASRG) and Advanced Stirling Convertor (ASC) projects. More information about the ASRG and ASC projects and the GRC role is available in References 1 to 6. One element of the GRC effort was an analytical creep life assessment of the ASC heater head (Fig. 1); it was performed to show that adequate margins exist on creep deformation and creep rupture for the long life times and demanding operating conditions of this application. There was uncertainty in the validity of the analytical assessment due to complexities of the material model and the creep life analyses for this MarM-247 component. To mitigate the risk of erroneous results, GRC planned a series of benchmark creep tests using full-scale heater head test articles. The test articles were subjected to high temperatures and to stresses ranging from nominal to approximately 40 percent higher, to create creep conditions similar to the ASC operating conditions. The resulting creep strains measured during testing were compared to predictions made using the analytical heater head creep models to verify the methodology.

Figure 1.—ASC-E2 heater head: The SN18 heater head test article after completion of permeability testing and removal of the permeometer flange hardware.

The first Microcast MarM-247 heater head test article of the ASC E2 design to undergo structural benchmark creep testing was recovered from a heater head specimen previously used in helium permeability testing; it was designated with the identification "SN18." This paper describes its use in pretest benchmark test rig preparations, wall thickness and diametral laser scan hardware developments, and custom induction heating coil experiments. The paper continues with the description and test results from the SN18 short benchmark test run, and finishes with a description of the use of SN18 in developing a unique temperature measurement methodology using contact thermocouples.

The usefulness of results from this testing was dependent on knowledge of the precise conditions under which the test article was subjected, namely the stress and temperature incident within the test article gage area where creep strain was measured. Accuracy of the stress field was determined by the precision of the test article diameter and thickness measurements, and by the use of high-precision calibrated transducers in the pneumatic pressurization system.

Accuracy of the variable temperature field is determined ideally with the application of very many weld-attached thermocouples to measure temperatures throughout the extended gage area. However, placement of welded thermocouples had negative consequences for this test method. Routing of the thermocouple wires and the associated insulators interfered with optical laser measurement of the test article strains. The insulating sleeves or thermocouples themselves may alter the temperature field resulting from the induction heating method in use. Moreover, thermocouple welds could alter local material creep properties. Finally and most importantly, it was discovered that the welds served as crack nucleation sites during fatigue loadings under some conditions. This fact resulted in the duration of the SN18 benchmark creep test being cut severely when crack growth from certain thermocouple welds caused excessive leakage of helium. Crack propagation from thermocouple welds was not experienced in earlier testing with the "Mooney 2-10" large-grain MarM-247 heater head test article (Ref. 7). The Mooney 2-10 test article was subjected to many pressure cycles during its benchmark creep test and was instrumented with a great many welded thermocouples. However, its geometry and material of construction were different from that currently proposed in the ASC program as well as actually incorporated in the SN18 test article. After the weld cracks limited SN18 to non-pressurized use, it was used to develop induction heating coil designs to provide desired heater head temperature gradient profiles and to measure those gage area temperatures with high spatial resolution. Later, SN18 was used with contact thermocouples to develop a unique temperature measurement methodology that eliminated the use of welded thermocouples in the pressurized region.

2.0 Structural Benchmark Creep Testing Overview

Structural benchmark creep testing provided high fidelity testing of prototypical heater head test articles and included the relevant material issues and multiaxial stress state in the test article creep response. The testing applied the design operating temperature profile for prototypical testing, or alternatively an accelerated "cascade" temperature profile (nearly constant high temperature maintained throughout the tapered wall gage area of a heater head test article) for more timely accelerated results, in a highly controlled laboratory environment. The test articles were pressurized with helium gas, thereby inducing a biaxial stress state very nearly the same as that in the complete ASC assembly heater head. Because the heater heads have tapered thickness walls, the stress magnitude varied by wall thickness in the gage area, even though the test article internal pressure was held constant. A schematic of the test setup is shown in Figure 2.

For accelerated testing using the cascade temperature profile, the thinner-wall, higher-stressed areas were temperature-accelerated (relative to the prototypical design temperature profile) to produce larger creep strains than nominal. The gage area of interest extended over most of the tapered wall due to capture the combined effect of elevated temperature and stress conditions. In the prototypical testing case, the critical creep strain measurement location was located at the thick end of the tapered wall, where higher creep strain rates existed due to high temperature, even though stresses were lower.

The heater head structural benchmark creep test facility included two test rigs. Each rig incorporated a digital control and data acquisition system, a bottle-fed closed high-purity helium pressurization system, an induction heater with custom copper coil or silicon carbide susceptor, a closed-loop cooling system, temperature sensing devices, and a pair of vertically translating laser micrometers. References 8 and 9 provide further discussion of the test apparatus and methods. For prototypical tests, the inductively heated susceptor was in a raised position, with the mounting manifold cooling water throttled to produce the design operating temperature profile to the extent possible. Strain measurements were concentrated at the critical location on the tapered wall. For accelerated testing, a bare induction coil was used at a lower level toward the tapered wall thin end, and laser scan measurements for calculation of diametral strains along the entire taper were of greater importance. During testing, the laser micrometers provided continuous strain measurement at discrete points, whereas intermittent full-length laser scans allowed creep characterization across the stress spectrum at selected time increments.

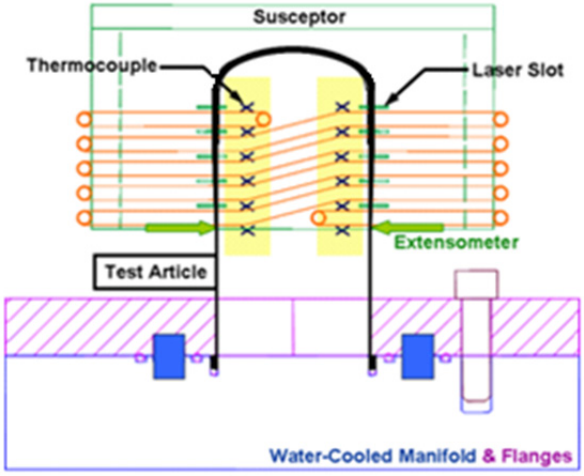

Figure 2.—Heater head benchmark creep test setup: schematic of an ASC heater head with an inductively heated susceptor and water-cooled base manifold-flange (bare coil inductor similar).

Accelerated benchmark creep testing was used to evaluate the effect of the biaxial stress field on creep response of the heater head, and it facilitated a comparison with the response predicted from accelerated uniaxial test data. In addition, the consequences of the MarM-247 grain microstructure on the thin wall creep response, the effects from potentially inhomogeneous heat treatment (if any) on creep deformation, and the detection of any circumferentially-directional creep caused by material processing or other mechanisms were investigated.

Both accelerated and prototypical benchmark testing creep strain results were compared to strains computed for the experimental conditions (including 3-sigma variations in temperature, pressure, and strain measurement) using procedures similar to those used for the heater head creep life assessment. If the cumulative creep strains fell within a three-sigma range of the calculated median value, indicating approximately 0.999 reliability, then the tests verified the heater head creep life assessment methodology. If the cumulative creep strains did not, re-investigation and fine-tuning of the analysis model would be called for to reflect more accurately the experimental setup and uncertainties. The heater head life assessment methodology then would be modified to incorporate any required systemic changes. Reference 10 presents a more complete description of the life assessment approach as well as an overview of heater head life criteria.

3.0 Origin of the SN18 Test Article

The SN18 test article was the first Microcast MarM-247 E2 design heater head to undergo permeability testing, which measures the rate that helium gas under high pressure passes through the thin walls (Fig. 3). After its use in the permeometer was complete, it was provided on August 7, 2008 as an early heater head benchmark test article to develop further the benchmark test methods and to obtain Microcast MarM-247 multiaxial creep test data. As received, the surface condition was questionable and had non-uniform oxidation; it was documented with photomicrographs, but no further analysis of the oxidation was performed.

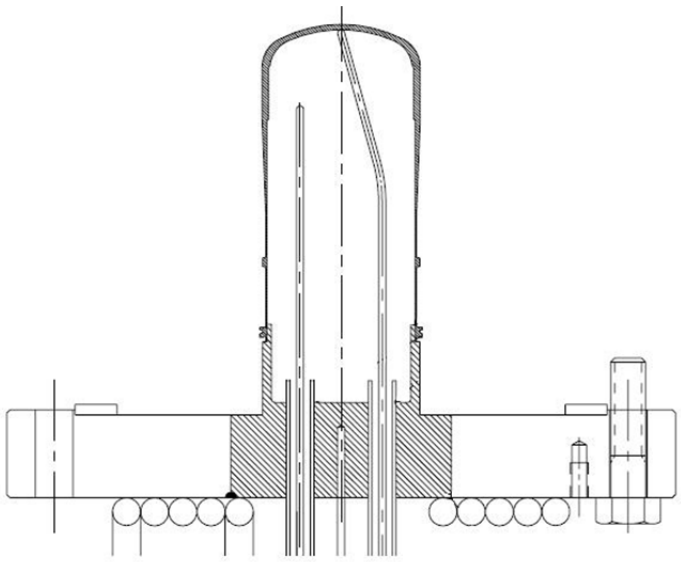

Figure 3.—Helium permeability test configuration: schematic of an earlier ASC heater head design with brazed-on permeometer mounting flange.

To separate the heater head from its permeometer flange, vacuum furnace de-brazing procedures were developed (Fig. 4). Two initial attempts at de-brazing in a furnace were made using a suspension wire and 70 lb of weight. The braze material melted away at 1100 °C, but the stainless steel inner permeometer mounting flange cylinder and the MarM-247 outer wall did not separate, possibly due to differential growth from the mismatched thermal expansion materials (Fig. 5). Additional attempts at separation were made at temperatures up to 1180 °C and with slots machined into the braze ring, along with other machined configurations, but, in the end, debrazing was not successful. Therefore, the bulk flange was separated from the heater head using precise electrical discharge machining. The remaining internal stainless steel ring was then completely removed, leaving a surface (Fig. 6) that could be sealed with the o-ring in the benchmark test rig manifold-flange.

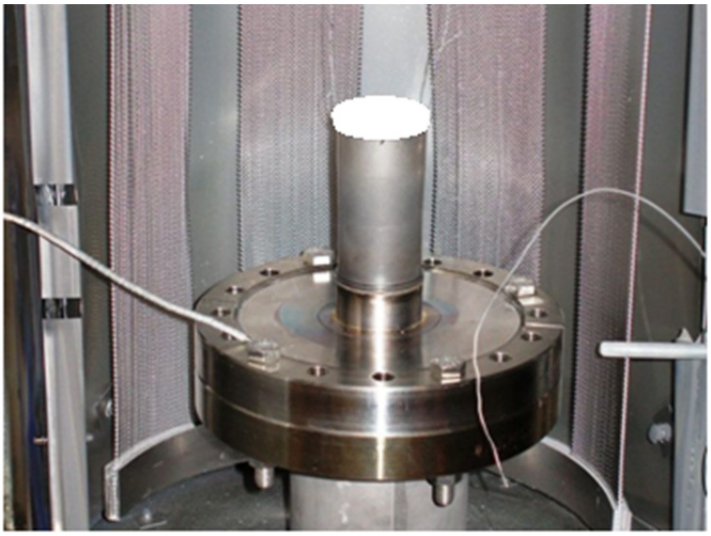

Figure 4.—SN18 in vacuum de-brazing furnace: Heating up to 1100 °C along with 70 lb of tensile force failed to separate SN18 from the permeometer flange brazed to the rejector end.

Figure 5.—SN18 heater head: Vacuum furnace de-brazing attempts failed to separate the heater head from its permeometer mounting flange.

Figure 6.—SN18 test article: Condition of rejector-end flange after removal of permeometer flange using electric discharge machining.

4.0 Benchmark Creep Test Preparation

Prior to starting the benchmark test of the SN18 heater head, it was check-fitted to the Benchmark Test Rig #3 hardware to assure that the newly exposed rejector end would fit into the rig manifold-flange and could maintain a pressure seal. After that was demonstrated, the test article was de-mounted, and precise room temperature wall thickness measurements were made using a fixture fabricated for that specific purpose; the fixture is shown in Figure 7. This fixture had a precision of 0.00005 in. (0.001 mm). The thickness measurements were made for 18 locations at each of nine axial positions (162 total distinct measurements) and were generally within the most stringent tolerance specified (Fig. 8). The primary purpose of the measurements was to enable accurate computation of benchmark test stresses for analysis of the benchmark test results and for validation of the probabilistic analytical assessment methodology. The as-built measurements also were used to determine orientation of the test article in Rig #3, so that creep strain behavior at the wall thickness extrema, i.e., local stress minimum and maximum locations, would be captured by the benchmark test instrumentation. Similarly, the measurements were used to determine where the diameter and profile laser scans would be taken.

Following the wall thickness measurements, the SN18 test article was instrumented with Type K welded thermocouples and additional gage area top and bottom extent markers, which were used to delineate clearly the gage area in laser scans. Next, calibrations of the two in-situ laser micrometers at benchmark test Rig #3 were verified using National Institute of Standards and Technology targets. Then, verification of calibrations was completed for the axial displacement sensors, linear variable differential transformers (LVDT's), using a very high precision, calibrated, electronic dial indicator. Finally, the test article was installed at the rig manifold-flange with an internal, high-purity, alumina volume plug, thermocouples were connected to the data acquisition system, and the high-purity helium pneumatic system was connected to the manifold.

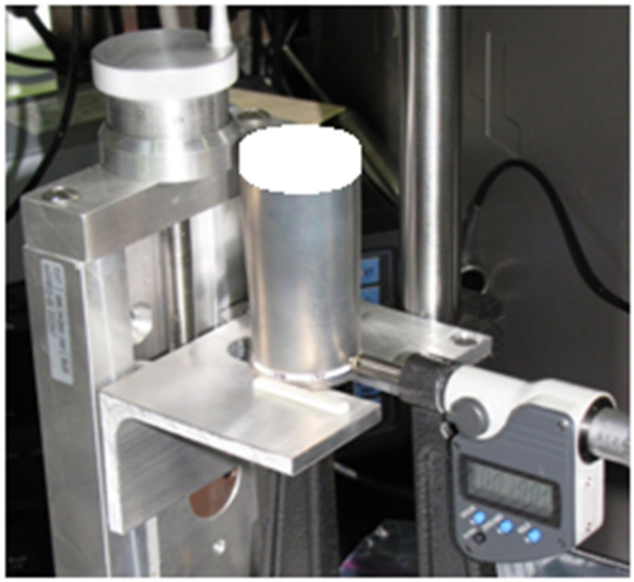

Figure 7.—Wall thickness measurements: A fixture was designed and fabricated to accurately measure heater head test article wall thicknesses at various axial positions.

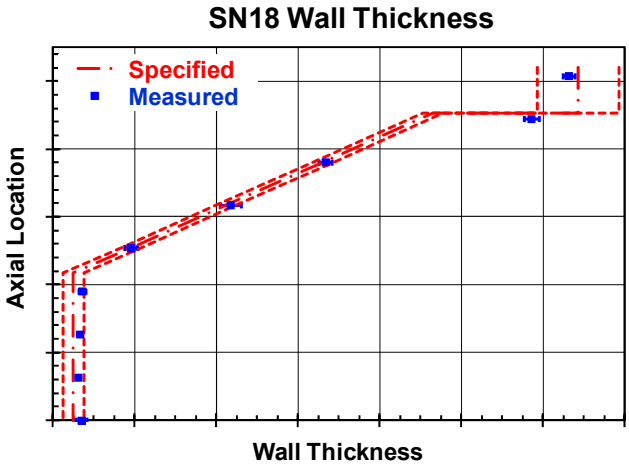

Figure 8.—SN18 wall thickness measurements: 162 measurements were made at nine total axial positions and generally were within the stringent fabrication tolerances.

Pretest preparations for the diametral scans were made using the X and Y in-situ lasers (Fig. 9). A study was completed to evaluate the effects on diameter measurement fidelity due to the internal laser scanning frequency and changes in internal averaging samples value, data acquisition rate, axial direction of scanning, and axial rate of scanning. Optimized settings resulted in scan noise levels approximately an order of magnitude better than the configuration used for previous benchmark creep testing. That facilitated interpretation of the elastic and creep response test data. Following the study, the diametral laser scans of the test article at room temperature and ambient pressure were completed. To measure the test article elastic strain response to pressure, SN18 was charged with the helium system up to the maximum test pressure, and in-situ scans again were completed at room temperature (Fig. 10). Note that this pressure is much higher than the heater head design peak (mean plus cyclic) pressure. Using the diametral laser scans from ambient and test pressures, the circumferential engineering strains in the gage area were calculated by dividing their difference by the original diameters. A plot of these measurements along with theoretical strains calculated by first principles is shown in Figure 11.

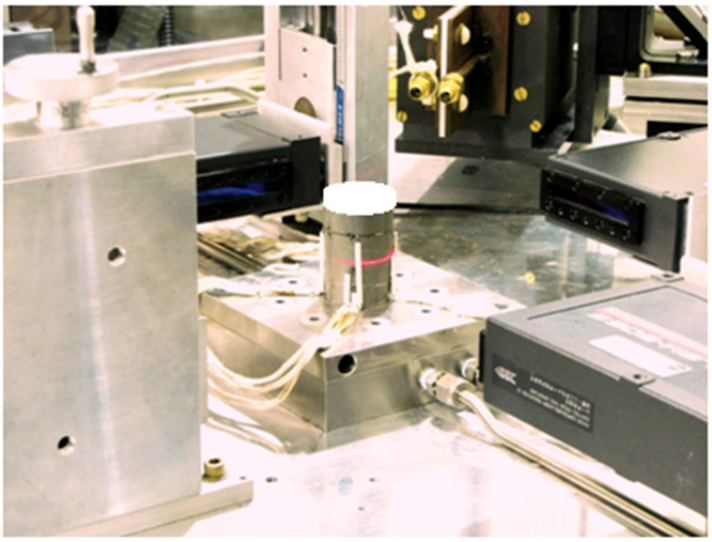

Figure 9.—In-situ laser scanning: SN18 was instrumented with thermo-couples, mounted to the Rig #3 manifold-flange, and scanned using in-situ laser micrometers.

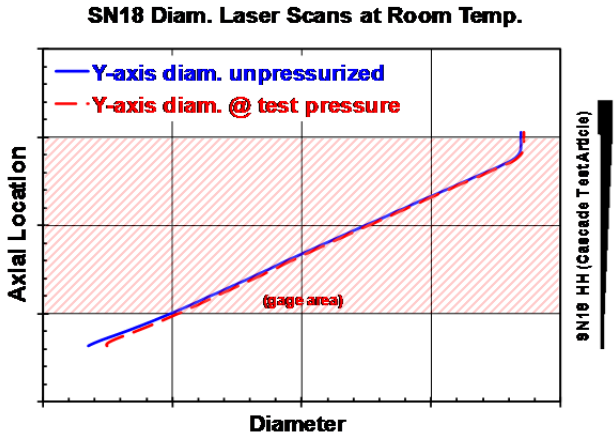

Figure 10.—SN18 diametral laser scans: In-situ laser micrometer scans of the test article relate outside diameter to axial position in the gage area (Y-axis scans shown at 0 and maximum test pressure).

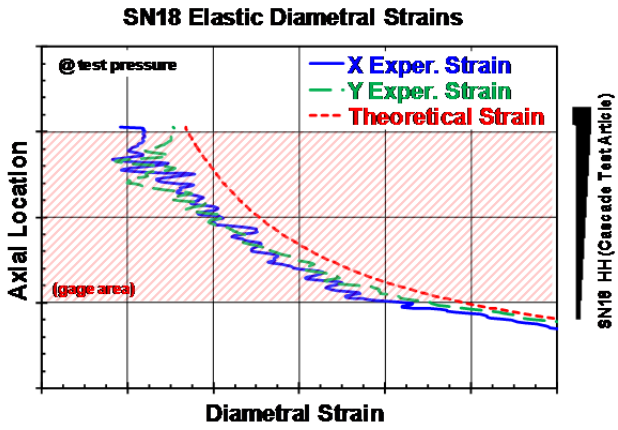

Figure 11.—SN18 experimental elastic strains: Diametral strains due to the test pressure are calculated from the diametral scans by dividing the difference of the 0 and maximum test pressure scans by the diameters obtained from the unpressurized scan.

To prepare for the SN18 benchmark creep test, temperature gradient experimentation using an inductively heated susceptor was performed with the #1B “Thermal Standard” at Rig #3. Various heating trials were conducted with the power source transformer traps, susceptor, coil, insulation, and geometry, seeking to optimize the accelerated “cascade test” temperature profile to be used for the test. It was found that the 3 kW power source could not drive the original silicon carbide susceptor to attain 850 °C over the desired gage area of the heater head (Fig. 12(a)). A new shorter susceptor with a double-wrap induction coil was fabricated and tested (Fig. 12(b)) but also failed to attain the 850 °C cascade profile. In fact, no coil configuration using a silicon carbide susceptor provided a heating gradient to overcome the water-cooled, cold-end heat sink and the natural effects of convective air cooling.

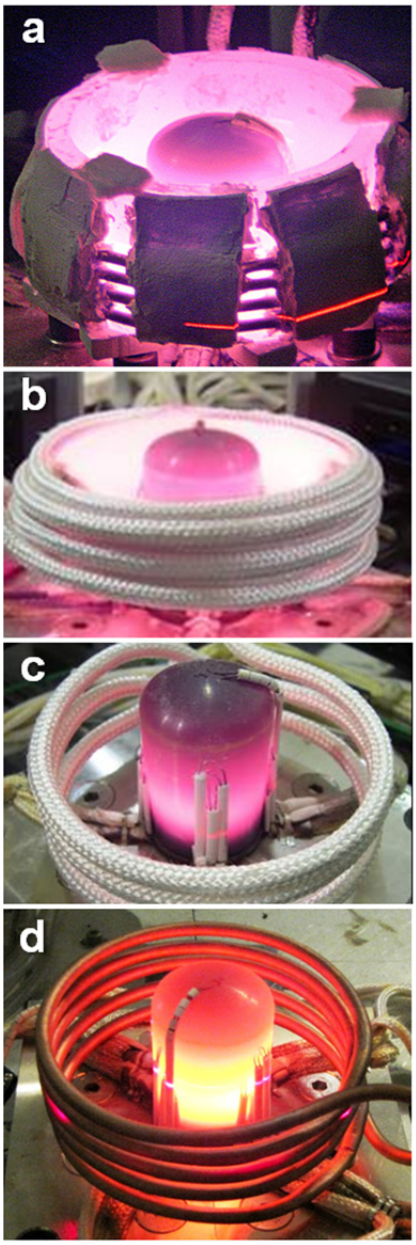

Figure 12.—Heating trials: To provide the flat cascade temperature profile, several induction configurations were tried.

With this experience, several bare induction coils were fabricated in an attempt to expand the temperature axial range while still providing the required uniform heating, the clearance for the micrometers' laser planes, and a margin on overheating the cold end o-ring seal. A three-turn coil (Fig. 12(c)) did not provide adequate induction. For the final, successful configuration, a bare, five-turn, copper tube induction coil was developed (Fig. 12(d)). This provided the best distribution of temperature over the length of the heater head tapered wall gage area. Based on the readings from 29 welded thermocouples on the Thermal Standard, the gage area temperatures were within 50 °C of the desired cascade profile for 80 percent of the gage area (Fig. 13). While the highly instrumented Thermal Standard was installed, three additional accelerated temperature gradients (at 825, 875, and 900 °C) were obtained for potential use in the SN18 heater head cascade test.

Pretest steady-state creep rate (SSCR) calculations were completed for the SN18 heater head test article to best predict the appropriate benchmark test internal pressure that would result in reaching the onset of tertiary creep for the most critical gage area location within the planned test duration of six months (Table 1). Both the ORNL master curve creep model and the simplified Arrhenius creep model were employed, using the test article's maximum principal stresses based on the precise test article wall thickness and the diameter measurements described previously. Results were determined for the experimental cascade temperatures measured from the Thermal Standard tests for the four temperature profiles with nominal values of 825, 850, 875, and 900 °C. The combination of the 850 °C profile at a medium high internal pressure was selected for the SN18 cascade benchmark test. Note that the SSCR calculations performed using the simplified Arrhenius creep model predicted smaller creep rates than those by the master curve creep model in these four cases. A comparison of the calculated SSCR's for the entire gage area using the master curve and Arrhenius creep models for the 850 °C profile is shown in Figure 14.

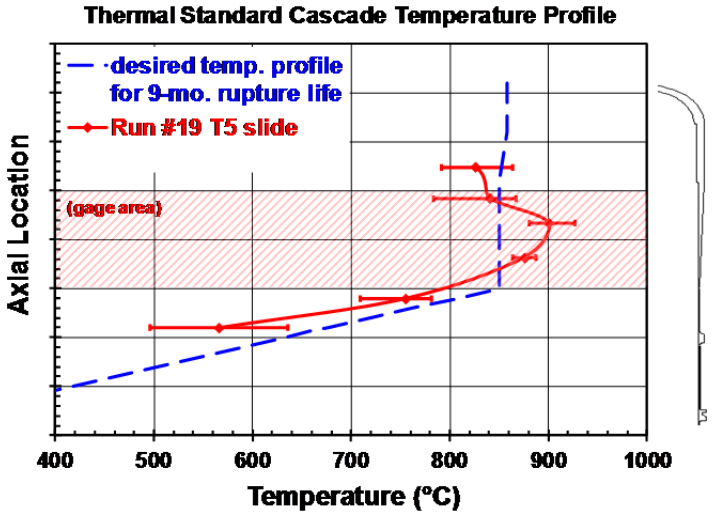

Figure 13.—Cascade temperature profile: Comparison of the measured temperature profile using a bare 5-turn coil with the #1B Thermal Standard, and the accelerated cascade temperature profile.

TABLE 1.—CALCULATED TEST PARAMETERS FOR CASCADE BENCHMARK CREEP TEST

Nominal cascade test temperature, °C	Heater head's internal pressure	Master Curve Model—Max. SSCR[a] (με/day)	Arrhenius Model—Max. SSCR (με/day)
825	high	80	30
850	med. high	80	26
875	med. low	80	15
900	low	80	6

[a]80 με/day steady state creep rate (SSCR) results in accumulated creep strain of 1.45% in six months

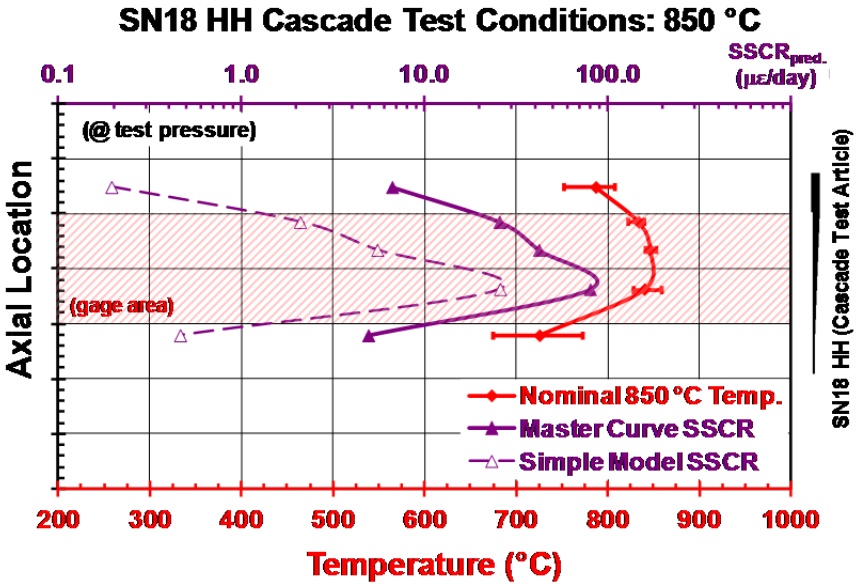

Figure 14.—Steady-state creep rate prediction for SN18: The master curve and simplified Arrhenius model creep rate predictions for the measured 850 °C cascade temperature profile of the Thermal Standard and the chosen medium high test internal pressure.

5.0 Benchmark Creep Testing and Results

Accelerated benchmark testing of the SN18 heater head test article began on April 3, 2009, using the nominal 850 °C cascade temperature profile and a medium high internal pressure (Fig. 15). As described previously, the MarM-247 master curve creep model was used with the calculated maximum principal stresses to predict that the onset of tertiary creep in the heater head gage area would began within the test period of six months. Before starting the SN18 test, the temperature profile was checked using a reduced number of thermocouples on SN18 (compared to the Thermal Standard) for identical heating settings obtained earlier using the Thermal Standard. The SN18 temperature profile closely matched that of the Thermal Standard but with slightly higher temperatures at the hot end of the gage area and slightly lower temperatures at the bottom, thinner-walled end. Using the master curve model to re-predict the creep response with the actual SN18 temperature profile, the result was that the maximum predicted steady state creep rate in the gage area was 48 microstrain per day, only 60 percent of the desired rate to complete the test in six months (Fig. 16). The changed temperature profile may have been a result of the difference in external geometry between the SN18 test article of ASC-E2 design and the #1B Thermal Standard test article of an earlier design, which had a different hot end configuration. A judgment was made to pursue the test with the obtained profile and to alter either temperature or pressure in the future if the observed creep rates were deemed too low. It was calculated that increasing the peak temperature approximately 18 °C would provide creep acceleration to restore the creep rate to 80 microstrain per day if needed.

In addition, before starting the SN18 test, several issues arose with new rig control software. This required that the heating system be controlled by one computer while most of the thermocouples be recorded on a separate computer. The arrangement degraded test article protection slightly, because, if limits set for permissive circuits including monitored thermocouples were exceeded, the controls would shut down the helium pressurization system but not the furnace. However, this would leave the test article in a safe state, with no applied mechanical stress or creep-inducing conditions. Nonetheless, surface oxide growth would continue and therefore add to the accumulated oxidation hours, which were being logged separately.

The SN18 test was interrupted after 73 hr duration to integrate fully the temperature recording and induction heater automated shutdowns with revised test control system software. Upon restart, the test ran without incident for a total of 187 hr. Using the scanning lasers in fixed position extensometer mode, real-time creep strain measurements were made at a critical position in the gage area; the measurements were corrected for the growth of an oxidation layer as described in the Appendix. The predicted creep rate at this location was 40 microstrain/day. The X-axis laser was discovered after test completion to have been influenced by thermocouple leads that displaced upon heating, interfering with the beam impinging on the test article outside wall. This led to incorrect results for the X-axis.

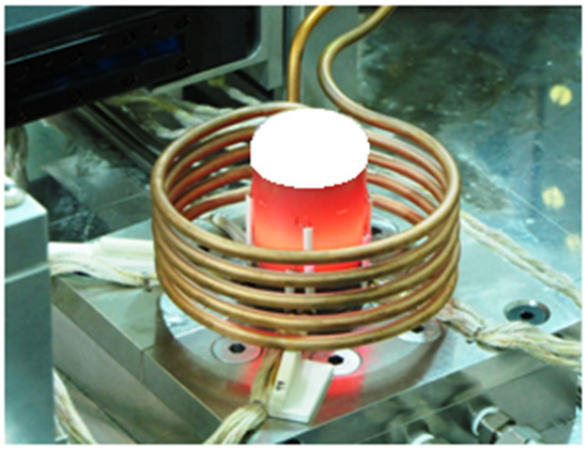

Figure 15.—SN18 structural benchmark creep test: This test started on April 3, 2009 using the five-turn bare coil and 850 °C cascade temperature profile with an applied medium high internal helium pressure.

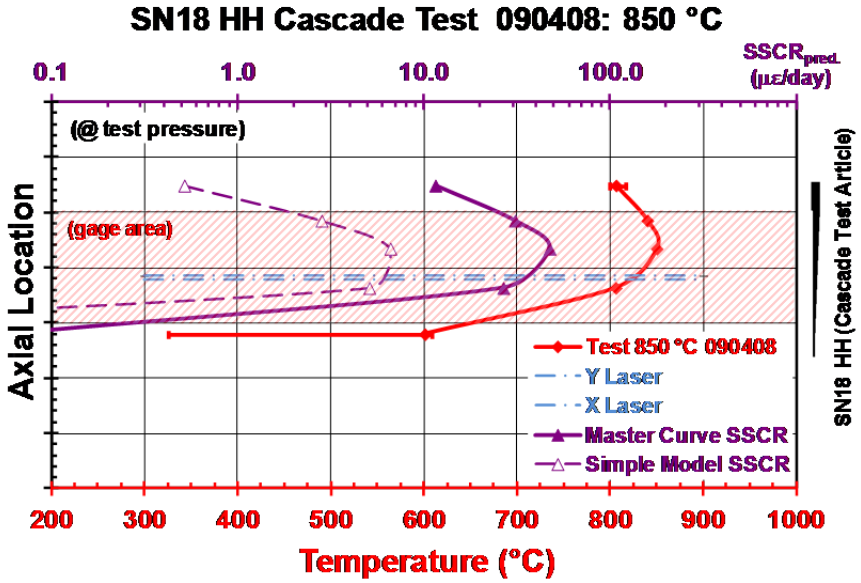

Figure 16.—Creep prediction for SN18 test temperatures: This revised creep rate prediction was made using SN18 measured temperatures.

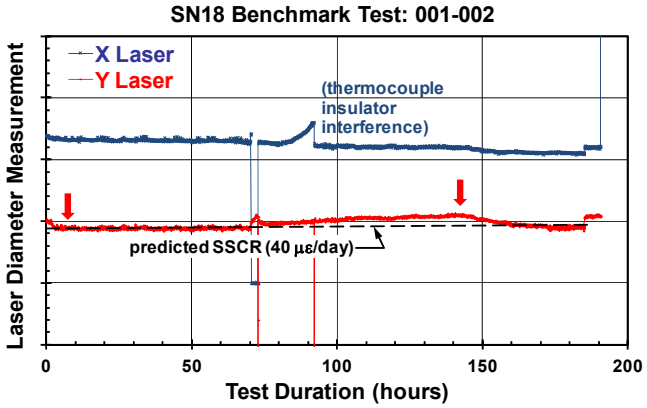

Figure 17.—Laser extensometer data for SN18 creep test: The Y-axis laser provided a signal indicating an average creep rate much higher than predicted; the X-axis reading may have been corrupted by interference from the thermocouple instrumentation.

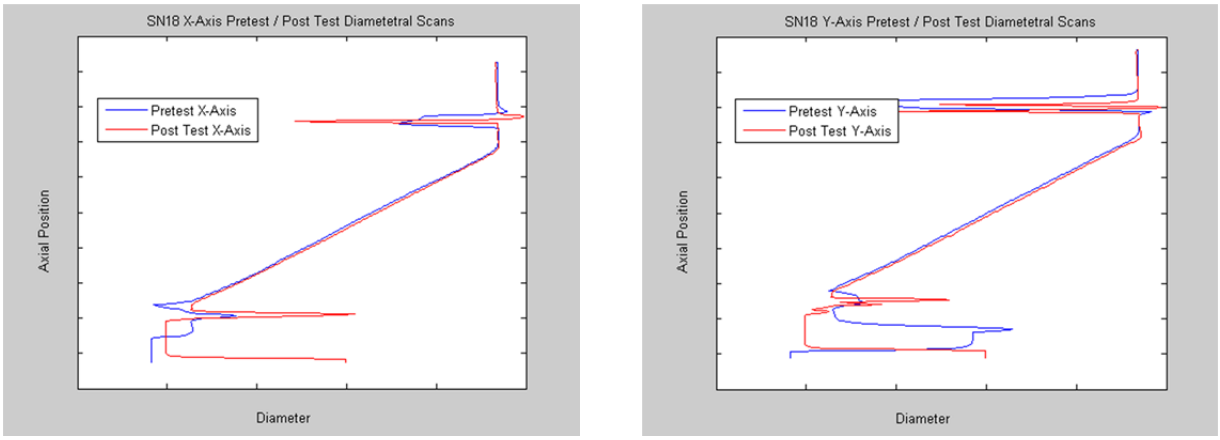

Figure 18.—SN18 diametral laser scans: Using scans from the in-situ laser micrometers, the pre- and post-test gage area diameter versus axial position plots are compared for SN18's X-axis (upper) and Y-axis (lower).

The test was terminated on April 13, 2009 to investigate increased consumption of helium gas; the accumulated total creep test time was 187.4 hr, and the total oxidation time was 190.4 hr. The Y-axis laser recorded a maximum creep strain rate that was significantly higher than the predicted rate (Fig. 17). The heating coil was removed and in-situ laser scans were completed to record the accumulated creep strains throughout the gage area (Fig. 18). Measurements were also recorded with the Instron uniaxial frame laser micrometer system to supplement the in-situ laser data. Similar to the calculation of elastic strains, the gage area creep strains where then calculated, but an allowance for oxide layer growth was subtracted from the post-test diameter data (Fig. 19). The analysis was performed using a Matlab script developed in-house, which permitted varied levels of smoothing but preserved the raw data for use in any future probabilistic analyses. Results of the analysis indicated that the maximum average X- and Y-axes creep strains and maximum average creep rates developed in the gage area were also higher than the prediction. In addition, the gage area maximums were somewhat greater than the stationary laser extensometers had measured, indicating that the extensometers were not positioned precisely at the location of maximum creep.

As previously described, the pre-test creep calculations predicted a maximum gage area SSCR of 48 microstrain/day, using the master curve creep law method. Although lower than the measured rate, this was quite an accurate prediction of the creep response, considering both the historically large scatter in experimental creep rates, and the fact that the measured creep rate may have included primary creep if it existed. Unfortunately, the test did not run long enough to distinguish a transition to a secondary, steady-state creep strain rate.

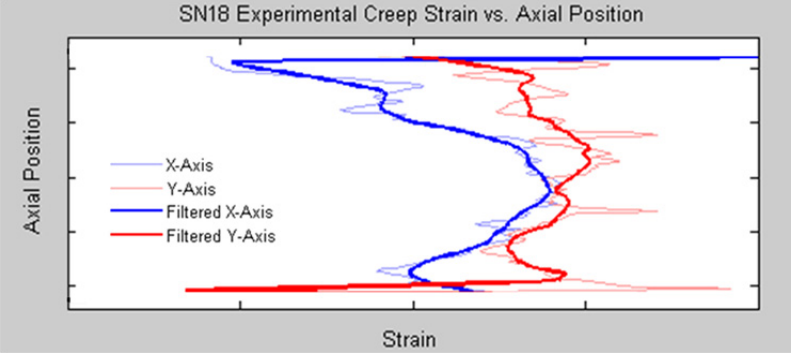

Figure 19.—SN18 Gage Area Creep Strains: Gage area creep strains were determined using Matlab, and they were significantly higher than predicted.

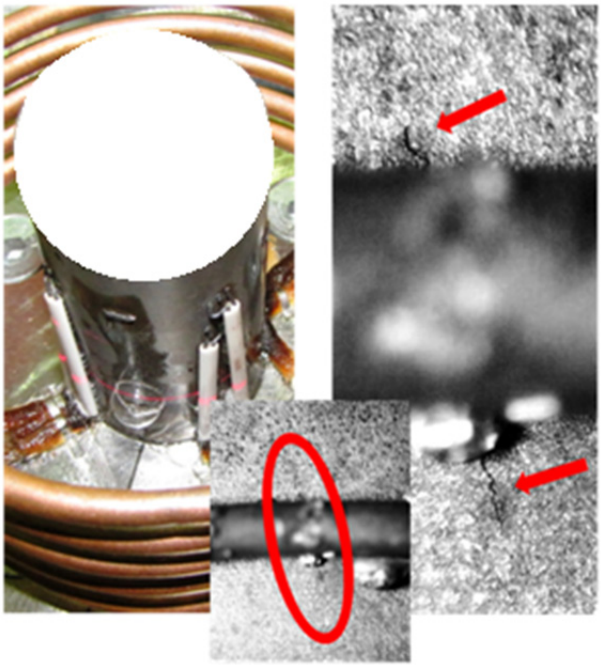

Figure 20.—Helium leaks at thermocouple welds: The growth of five cracks at these locations led to termination of the SN18 benchmark creep test.

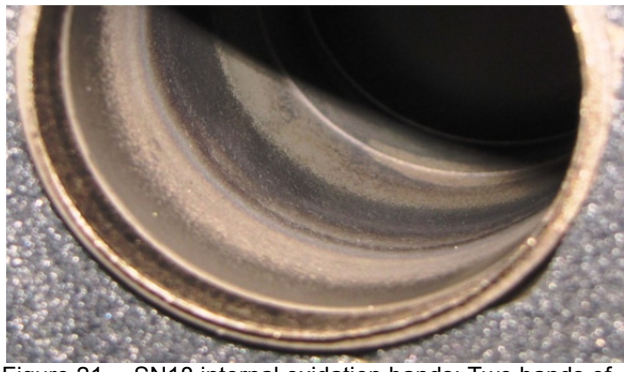

Figure 21.—SN18 internal oxidation bands: Two bands of increased oxidation were observed at areas with temperatures of 200 to 400 °C and 800 to 850 °C.

The increased consumption of helium gas in the test was investigated and found to be leakage of helium through the test article thin walls at thermocouple locations. Optical microscopy was used to detect five through-thickness cracks in the test article (Fig. 20). All cracks initiated at thermocouple or gage-area-marker weld locations on a plane just below the gage area; the cracks had propagated up to one millimeter in length. At this location, the temperature was 600 °C, and the tapered wall thickness was small, resulting in a high stress level. Because of their location and spacing, it is believed that the presence of these defects did not affect the test article strain measurements.

Due to the observed rapid progression of crack growth during the five cycles of full pressurization that SN18 endured, it is felt that the five cracked areas must be not only sealed, but also structurally reinforced, if any future creep testing with this test article is to be performed. Inspection of the interior surfaces of SN18 showed two bands with slightly increased oxidation. The bands corresponded approximately to temperature ranges of 200 to 400 °C and 800 to 850 °C (Fig. 21). The internal environment of the test article during testing had very low oxygen content, as the test procedures included

vacuum purging several times and the use of high-purity helium gas. The oxidation was thought to have negligible effect on creep response of the test article.

Additional benchmark creep testing of the SN18 test article was not performed due to the need to make wall repairs, the likelihood that further cracking would occur at other welds, and constraints of the project schedule. The test article was used productively as a thermal standard for a subsequent heater head benchmark test (Ref. 11), and for an extensive study to develop a contact thermocouple procedure that eliminated use of welded thermocouples for heater head temperature measurement (Ref. 12).

6.0 Summary

The Glenn Research Center conducted an analytical creep life assessment of the heater head component of the Advanced Stirling Convertor for the Lockheed Martin Advanced Stirling Radioisotope Generator. This life assessment defined several creep response criteria to substantiate component lifetime based on computational results that relied on material creep properties derived from uniaxial creep testing of the heater head material. The heater head component was required to meet the creep criteria with high reliability as determined by probabilistic analysis. Due to the complexity of the creep life assessment, a heater head structural benchmark creep testing program was established to validate this methodology.

The SN18 test article was an early benchmark creep test article salvaged from a previously completed helium permeability test. It served as a useful tool to develop structural benchmark creep testing methods and to provide the first multiaxial creep test results for the Microcast MarM-247 material, the heater head material of construction. The use of SN18 minimized potential negative effects on test results from initial future creep test articles of much higher value. It also instigated development of a new temperature measurement technology that replaced otherwise overly intrusive and damaging thermocouple instrumentation. Creep results from the SN18 test article under the imposed accelerated cascade test conditions provided the first verification of the analytical life assessment procedures within expected experimental noise. The SN18 benchmark creep testing experience proved to be important and valuable.

References

1. Chan, Jack, Wood, J. Gary, and Schreiber, Jeffrey G.: Development of Advanced Stirling Radioisotope Generator for Space Exploration. NASA/TM—2007-214806, 2007.
2. Shaltens, Richard K., and Wong, Wayne A.: Advanced Stirling Technology Development at NASA Glenn Research Center. NASA/TM—2007-214930, 2007.
3. Wong, Wayne A., Wood, J. Gary, and Wilson, Kyle: Advanced Stirling Convertor (ASC) - From Technology Development to Future Flight Product. NASA/TM—2008-215282, 2008.
4. Schreiber, Jeffrey G. and Thieme, Lanny G.: GRC Supporting Technology for NASA's Advanced Stirling Radioisotope Generator (ASRG). Proceedings of the Space Technology and Applications International Forum (STAIF-2008), edited by M.S. El-Genk, American Institute of Physics Conference Proceedings 969, Melville, New York, 2008, pp. 582-592.
5. Wong, Wayne A., Wilson, Kyle, Smith, Eddie, and Collins, Josh: Pathfinding the Flight Advanced Stirling Convertor Design with the ASC-E3. Proceedings of the 10th International Energy Conversion Engineering Conference, AIAA-2012-4251, American Institute of Aeronautics and Astronautics, Reston, VA, 2012, pp. 1-10.
6. Lewandowski, Edward J.: Testing of the Advanced Stirling Radioisotope Generator Engineering Unit at NASA Glenn Research Center. Proceedings of the 10th International Energy Conversion Engineering Conference, AIAA-2012-4253, American Institute of Aeronautics and Astronautics, Reston, VA, 2012, pp. 1-11.
7. Krause, David L.: Results for Structural Benchmark Creep Testing of a Large Grain MarM-247 Advanced Stirling Convertor Heater Head Test Article. NASA/TM—2009-215620, 2009.

8. Krause, David L., Kalluri, Sreeramesh, Bowman, Randy R., and Shah, Ashwin R.: Structural Benchmark Creep Testing for the Advanced Stirling Convertor Heater Head. Proceedings of the 6th International Energy Conversion Engineering Conference, AIAA 2008-5774, American Institute of Aeronautics and Astronautics, Reston, VA, 2008, pp. 732-741.
9. Krause, David L., Kalluri, Sreeramesh, and Bowman, Randy R.: Structural Benchmark Testing for Stirling Convertor Heater Heads. Proceedings of the Space Technology and Applications International Forum (STAIF–2007), edited by M.S. El-Genk, American Institute of Physics Conference Proceedings 880, Melville, NY, 2007, pp. 297-304.
10. Shah, Ashwin R., Korovaichuk, Igor, Krause, David L., and Kalluri, Sreeramesh: Advanced Stirling Convertor Heater Head Durability and Reliability Quantification. Proceedings of the 6th International Energy Conversion Engineering Conference, AIAA 2008-5772, American Institute of Aeronautics and Astronautics, Reston, VA, 2008, pp. 167-174.
11. Krause, David L.; Kalluri, Sreeramesh; Shah, Ashwin R.; and Korovaichuk, Igor: Experimental Creep Life Assessment for the Advanced Stirling Convertor Heater Head. Proceedings of the 8th International Energy Conversion Engineering Conference, AIAA Conference Proceedings 2010-7093, Reston, VA, 2010.
12. Brewer, Ethan J., Pawlik, Ralph J., and Krause, David L.: Contact Thermocouple Methodology and Evaluation for Temperature Measurement in the Laboratory. NASA/TM—2013-216580, 2013.

Appendix—Correction of Creep Strain Measurements for Oxidation Layer Growth

Structural benchmark creep testing of heater heads was performed at high temperature and in air, subjecting the test articles to an oxidizing environment. For the ASC heater heads fabricated from MarM-247, the exterior test article surfaces oxidized slightly; the growth of this oxidation layer was accounted for when calculating heater head creep strains based on optical laser measurements of the test article diameters.

To quantify the MarM-247 oxidation layer growth over time, a small experimental study was completed. Based on the ready availability of materials, one large-grain MarM-247 and two Microcast MarM-247 rectangular oxidation specimens were exposed to an 850 °C air environment in a metallurgy furnace. One large-grain MarM-247 specimen was held at ambient conditions and served as a control specimen. A plot of the results from measurements made over the exposure period of 5036 hr is shown in Figure 22.

When diametral laser measurements of heater head test articles were made, the total exposure time was noted, and the average oxidation layer thickness measured in this study for that exposure time was subtracted from each radius; the resulting difference was the test article diameter corrected for oxidation layer growth. When the original, unexposed test article diameter was subtracted from this number, and then divided by the original, unexposed diameter, a measure of the creep strain was obtained that was corrected for oxidation layer growth.

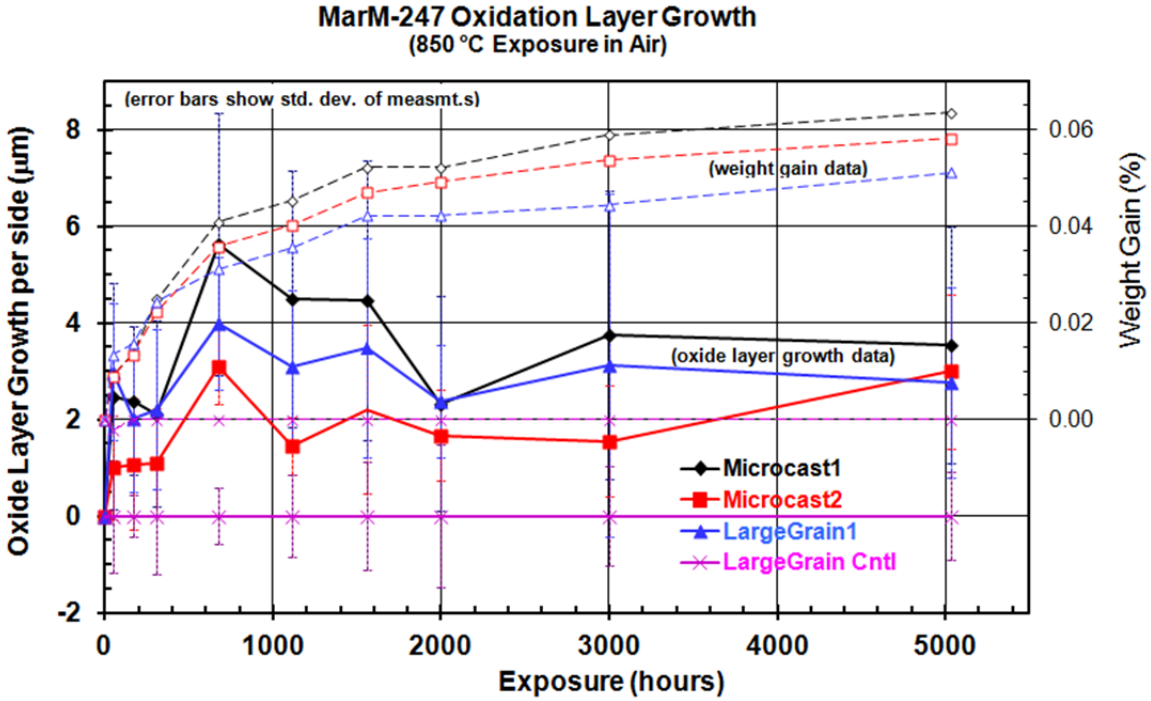

Figure 22.—MarM-247 oxidation layer growth: Results from measurements of oxidation layer growth of MarM-247 during exposure to air at 850 °C.